JMEPEG (2009) 18:38–48
DOI: 10.1007/s11665-008-9265-x

1059-9495/$19.00

Fine and Ultrafine Particle Characterization and Modeling in High-Speed Milling of 6061-T6 Aluminum Alloy

Imed Zaghbani, Victor Songmene, and Riad Khettabi

(Submitted May 22, 2008; in revised form June 4, 2008)

In this study, an experimental investigation was carried out on fine and ultrafine metallic dust emission during high-speed milling of 6061-T6 aluminum alloy in wet and dry conditions. Measurements of dust emission were conducted using a scanning mobility particle sizer spectrometer and an aerodynamic particle sizer spectrometer. These instruments were used to characterize particles in the micrometer and the nanometer size ranges. It was confirmed that the machining process produces nanoparticles as small as 10 nm and that the characteristics of the generated nanoparticles are not significantly influenced by the cutting conditions. The cutting forces and chip compression ratio were measured to validate the proposed dust generation model based on an energy approach. Good agreement was observed between the model and the experimental measurements for the investigated conditions. It was demonstrated that the majority of generated dust is caused by deformations in the primary shear zone. In addition, the percentage of generated dust is significantly influenced by deformation conditions in the chip formation zone. It was found that high cutting speeds could reduce the percentage of the generated particles during the milling process.

Keywords clean machining, dust modeling, microparticles, nanoparticles, orthogonal milling

1. Introduction

The machining process is a widely used technique for shaping of metallic and nonmetallic materials. In spite of the multiple advantages of machining, it is considered hazardous for operators and for the environment. In fact, most machining processes generate aerosols in liquid or solid forms. One of the best strategies for reducing the impact of this hazard on worker health and the environment is reduction of dust generation at the source. To accomplish this, there is a need to understand the conditions governing the production of dust during machining processes.

Since 1980, some interesting findings have already been observed regarding machining dust. It was found that the intensity of dust formation increases with an increase in cutting speed during turning and milling of almost all brittle materials (Ref 1). The dust formed when machining iron, steel, and brass at higher speeds has a much larger percentage of particles below five microns in size. It has also been confirmed that the use of fluids can reduce dust formation by ~40-50%, (Ref 1). Tönshoff et al. (Ref 2) showed that, during grinding, most metallic dust generated is breathable, and, without a dust suction system, the level of dust particle concentration in the air is higher than the threshold fixed by the NAOSH regulations (North American Occupation Safety and Health). For processes such as drilling and turning, some remarkable work has been produced. The quantity and particle size of machining dust were found to be dependent on cutting parameters, tool material, work piece material, and tool geometry (Ref 3). In addition to the cited factors, lubrication has a direct impact on the quantity and size of the produced particles. While comparing the aerosols released during dry and wet turning, Sutherland et al. (Ref 4) found that the quantity of mist and dust produced during machining increases with the speed, the feed, and the cutting depth. For the investigated conditions, the authors found that a large percentage of the 1-4 μm size particles were produced during dry machining, while the great majority of the particles produced during wet machining were below 1 μm. Ramulu et al. (Ref 5) commented that dust generated during the machining process can affect the torque during a drilling process of graphite-bismaleimide composite material.

All of these results lead to the conclusion that machining dust is related directly to the chip formation process. This conclusion is confirmed by experimental studies in Ref 6 and 7, where the fundamental causes of the production of dust during dry drilling processes were studied. Light materials (aluminum alloys and magnesium alloys) were drilled under different machining conditions, and their effect on fine dust generation was studied. Chip formation phenomenology was used to explain the observed results, and interesting explanations were proposed.

It is known that some particle size ranges are more dangerous than others. The toxicity of metallic dust depends on size and composition. Particles with sizes between 2.5 and 10 μm remain in the trachea and bronchioles, while those larger than 10 μm settle in the nose and the thorax. These last particles are the least dangerous and are normally expelled naturally from the human body. When operators breathe in manufacturing dust (metallic particles, oxides, fluid mixed with air, etc.), the large particles segregate in the respiratory parts of the body (nose, throat, larynx), and the medium-sized particles enter the lungs. The fine particles (less than 2.5 μm) can go as far as the alveoli and the deepest parts of the lung (Ref 8), where such exposure can generate health problems

Imed Zaghbani, Victor Songmene, and **Riad Khettabi**, ETS – Mechanical Engineering, University of Quebec, Montreal, QC, Canada. Contact e-mail: victor.songmene@etsmtl.ca.

ranging from respiratory diseases to asthma and several types of cancer.

Following the work of Witschger et al. (Ref 9), the two particle size ranges that should be observed carefully are the 1-2.5 μm and the 10-20 nm size ranges because these particles are considered the most dangerous. Machining dust in the 1-2.5 μm size range has been explored in many papers; however, the 10-20 nm size range is not yet well characterized, according to the author's knowledge.

Some recent findings show that nanoparticles can be as harmful as microparticles when absorbed by body cells (Ref 10). Oberdörster et al. (Ref 11) proved with experimental studies that some inert particles could become biologically active when their dimensions are reduced to the nanometer scale. Witschger et al. (Ref 9) found that the particle aerodynamic diameter has an impact on the pulmonary deposition site. Ostiguy (Ref 12) stated that the first particularity of nanoparticles is their pulmonary deposition modes, which are different from and more dangerous than the deposition modes of microparticles. Nanoparticles can migrate along the olfactory nerve (Ref 13) and penetrate the central neural system, eventually reaching the brain (Ref 14). Gatti (Ref 15) confirmed that some nanoparticles were found in liver, kidney, and other organs (i.e., micro- and nano-debris of exogenous origin). Elder et al. (Ref 16) proved that nanoparticles toxicity is in direct relation to their number and specific surface, and not only a function of their mass concentration as for microparticles.

Most of the existing studies that cover machining dust are generally limited to aerodynamic diameters greater than one micron. With the recent results published on nanoparticles and how harmful they may be, more interest should be given to machining dust in the nanometer scale. It is therefore necessary to know all the size ranges of particles produced during normal machining processes and their different properties.

Published works found in the literature on machining dust were carried out on turning (Ref 3, 4) and on drilling (Ref 6, 7-17) processes. The studied cutting speeds were low or moderate, not exceeding 400 m/min. Some works have been done in the wood-milling field (Ref 18) and for medium-density fireboard material milling (Ref 19). However, little is known about machining dust generation during high-speed milling of metals. The main aim of this work is to study the generation of microparticles and nanoparticles during dry and wet milling processes at high cutting speeds ranging from 300 to 900 m/min. In addition, a dust generation model for microparticles is proposed for dry and wet milling.

To conduct measurements and model validation, a new experimental setup is proposed with two combined measurement instruments designed to explore the microparticle and nanoparticles domains. The instruments used are an aerosol particle sizer spectrometer (APS^{TM}) and a scanning mobility particle sizer spectrometer (SMPS^{TM}).

The paper is organized as follows: in the first section, the methodology is presented starting with details of the proposed model for dust generation, then the experimental setup designed to study fine and ultrafine dust generation during milling processes is explained, and finally the proposed design of experiments is covered. In the second section, the results for microparticles are presented, followed by findings on the nanoparticles. In the next part, model validation is illustrated, followed with comments and discussions. In the last section, important conclusions found in the study are summarized.

2. Method and Procedure

2.1 Dust Generation Modeling

Khettabi et al. (Ref 3) proposed an empirical model for microparticle dust emission during turning processes using the following empirical relation:

$$D_u = \frac{A}{V_c^m \exp\left(\frac{BV_0}{V_c}\right)} \quad \text{(Eq 1)}$$

where D_u is the chip fraction that becomes dust during the chip separation, V_c is the cutting velocity, and A, B, and m are empirical constants. Rautio et al. (Ref 19) also used a similar fraction to study the dust emission during milling of medium-density fiberboard materials. It was pointed out that there are various causes for dust production during machining such as chip deformation, tool-chip friction, and tool-work piece friction (Ref 6, 7-17). In all of these sources, the primary shearing zone is believed to be the main source because it is the main deformation zone. In a recent study, Khettabi (Ref 20) expected that the amount of dust is related to the amount of energy created in the chip formation zone. The expected dependency was expressed using the following equation:

$$D_u = \frac{A}{V_c^m \exp\left(\frac{E_a}{E_s}\right)} \quad \text{(Eq 2)}$$

where E_a is the average activation energy of the work piece material and E_s is the deformation energy in the chip formation zone; V_c is the cutting velocity and A is the material constant. In the present study, the proposed formulae in Eq 2 will be used. If it is assumed that the majority of generated dust is created in the primary shear zone, the deformation energy in the chip formation zone E_s can be limited to the energy in the primary shear zone. For an orthogonal cutting process, the energy expended per unit area, E_s, is defined in Ref 21 using the following equation:

$$E_s = V_{sh}\tau_{AB}\sin\phi \quad \text{(Eq 3)}$$

where V_{sh} is the shear velocity, τ_{AB} is the shear stress in the primary shear zone, and ϕ is the shear angle. Using Eq 2 and 3, the following equation can be used to predict the fraction of the generated dust emission during an orthogonal milling process:

$$D_u = \frac{A}{V_c^m}\exp\left(\frac{-E_a}{\left(1-\frac{\sin\alpha_n}{C_h}\right)\tan\phi V_c\tau_{AB}}\right) \quad \text{(Eq 4)}$$

where C_h is the chip compression ratio, α_n is the tool rake angle, and τ_{AB} is the shear stress (other parameters are the same as in Eq 2). To predict the dust emission as a function of the cutting parameters (in addition to the work material and the tool geometry), the following parameters should be estimated: the chip compression ratio C_h, the shear angle ϕ, and the shear stress τ_{AB}.

The chip compression ratio, C_h, is measured experimentally using the procedure described in section 2.2. From the estimation of C_h, the shear angle ϕ can be estimated in terms of rake angle, α_n, using the following equation (Ref 22):

$$\tan\phi = \frac{\frac{\cos\alpha_n}{C_h}}{1 - \frac{\sin\alpha_n}{C_h}} \quad \text{(Eq 5)}$$

The shear stress, τ_{AB}, is calculated from the measured cutting forces using the following formula (Ref 23)

$$\tau_{AB} = \frac{\sin\phi}{wf}\left(\overline{F}_y\cos\phi - \overline{F}_x\sin\phi\right) \quad \text{(Eq 6)}$$

where $\overline{F}_x$ and $\overline{F}_y$ are the average cutting forces measured in the x and y directions, w is the axial depth of cut in mm, and f is the feed in mm/tooth. The procedure used for estimating D_u for a given set of cutting conditions is as follows:

Step 1: Choose five cutting conditions for identification of the model constants (A, E_a, and m).
Step 2: Measure the average cutting forces $\overline{F}_x$ and $\overline{F}_y$. Measure the total generated dust for the 0.5-10 micron size range.
Step 3: Collect some of the chips generated during the milling process.
Step 4: Measure the step length L_c under an optical microscope (see Fig. 3) and calculate the chip compression ratio C_h ($C_h = L_1/L_c$).
Step 5: Estimate the shear angle ϕ using Eq 5.
Step 6: Estimate τ_{AB} using Eq 6.
Step 7: Use the Levenberg-Marquadt algorithm to identify the constants E_a, A, and m.
Step 8: Calculate D_u using Eq 4.

2.2 Experimental Measurements

2.2.1 Sampling Methods. Two spectrometers were used to measure the machining dust characteristics: an aerodynamic particle sizer spectrometer (APS^{TM}) and a scanning mobility particle sizer spectrometer (SMPS^{TM}).

The APS^{TM} instrument (Model #3321, TSI, Inc.) is based on time-of-flight particle sizing technology which involves measuring the acceleration of aerosol particles in response to the accelerated flow of the sample aerosol through a nozzle. The aerodynamic size of a particle determines its rate of acceleration, with larger particles accelerating more slowly due to increased inertia. As particles exit the nozzle, the time-of-flight between the model 3321's two-laser beams is recorded and converted to an aerodynamic diameter using a calibration curve (Ref 24).

The SMPS^{TM} instrument consists of an electrostatic classifier (model #3080 TSI, Inc.) and an ultrafine water-based condensation particle counter UPWCPC (model #3786, TSI, Inc.). The model 3080 Electrostatic Classifier consists of a Kr-85 bipolar charger used to neutralize the charges on particles, a controller to control flows and high-voltage, and a differential mobility analyzer (DMA), which separates particles based on their electrical mobility. The separated particles are counted with the UPWCPC (TSI Inc. 2008) (Ref 25). The UWCPC is a water-based condensation particle counter designed to measure the concentration of airborne ultrafine particles. The UWCPC draws in an air sample and counts the number of particles in that sample to provide a particle concentration value that is displayed as the number of particles detected per cubic centimeter of sampled air. The UWCPC uses a laser and an optical detector to detect the particles, passing the sampled flow through a viewing volume illuminated by a laser. The instrument relies on a condensation technique to deposit a working fluid on the particle to amplify the size to a value that can be detected readily with a conventional optical system (Ref 26).

2.2.2 Experimental Setup. The experimental setup for measuring the dust emission during orthogonal milling process is presented in Fig. 1 and 2. The workpiece (3) was attached to a steel support (2) clamped rigidly to a three-component dynamometer (1). The assembly was insulated using a G-Class Plexiglas box (6). The dust measurement units (SMPS^{TM}-APS^{TM} instruments) were connected to the insulated assembly through a 10 mm diameter tube (7) plugged into the Plexiglas box. The air suction hole was positioned as near as possible to the cutting zone, as shown in Fig. 2.

The inlet flow rate was set to 2.8 L/min. The aspirated air is divided into two flows: the first flow is used to analyze microparticles (size range 0.5-20 µm) in the APS^{TM} (8), and the second flow is used to analyze the nanoparticles (size range 10-736 nm) in the SMPS^{TM} (9). Air aspiration is started up at the beginning of the milling test and is stopped 5 min after test completion. This procedure was applied for each test so that the measurements take place during and after the machining operation.

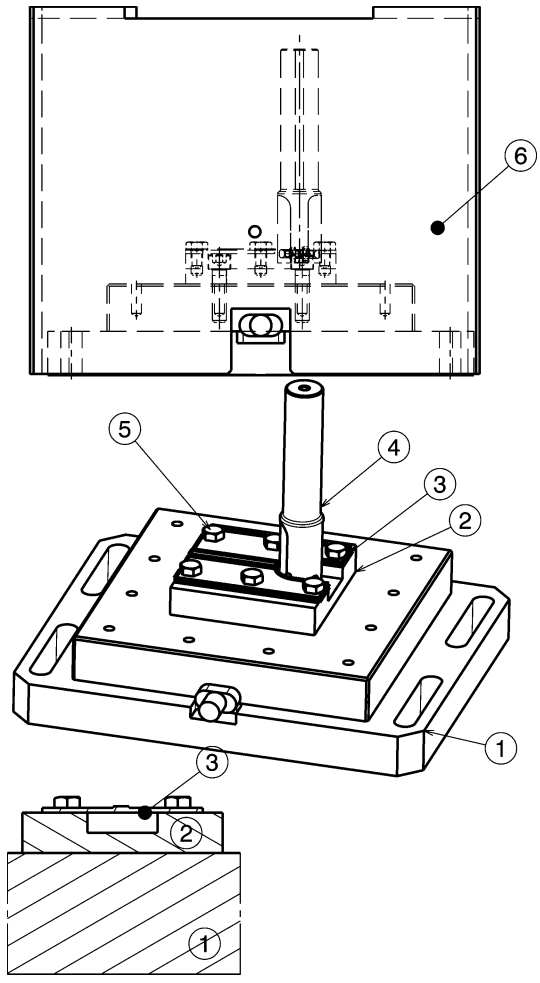

Fig. 1 Experimental setup design for measuring machining dust during orthogonal milling process—1: Three axes dynamometer; 2: Support; 3: 6061-T6 aluminum workpiece; 4: Cutting tool; 5: Fixture screw; and 6: dust cover

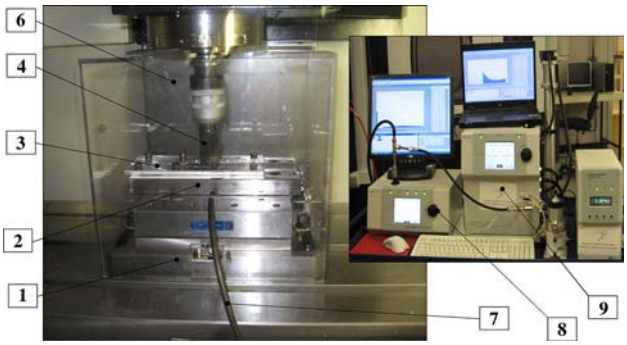

Fig. 2 Setup for dust collection and measurement—1: Three axis dynamometer; 2: Support; 3: 6061-T6 aluminum workpiece; 4: Cutting tool; 6: Dust cover; 7: Air suction tube: 8: APS^{TM}; 9: SMPS^{TM}

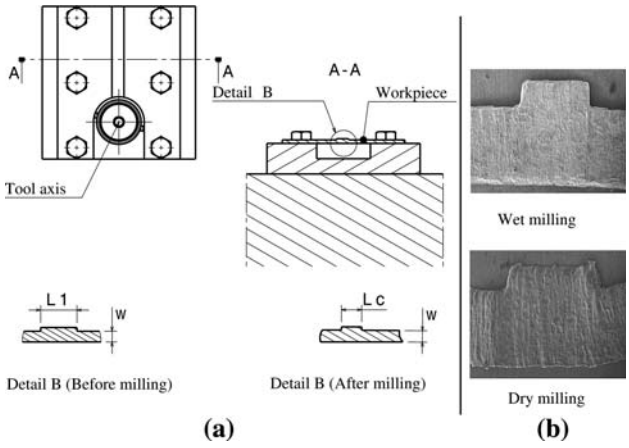

Fig. 3 Method for measurement of the chip compression ratio C_h: (a) L_1 is the initial chip length ($C_h = L_1/L_c$) and (b) Two samples of collected chips for different cutting conditions

A three-component dynamometer (Kistler 9255B) was used to measure the cutting forces in the x and y directions, and the average cutting forces were recorded for each test. The generated chips were collected and used to estimate the chip compression ratio C_h. Figure 3 illustrates the method used to calculate the ratio C_h; this method was adopted from Ref 27. Each chip was observed under an optical microscope, and the width w and the length of the compressed step L_c were measured.

A 38.1 mm diameter tool was used during all machining tests (KISZ1.5P2.53L905). The cutter has two inserts; only one insert was used, and the second one was ground to ensure orthogonal cutting conditions. The inserts used during the machining test were coated and designed for machining aluminum alloys (XPMT2533L-K725M), and were chosen without a chip breaker to minimize chip fragmentation for easier manipulation and measurement.

2.3 Design of Experiments

Table 1 summarizes the experimental conditions considered in this study. The same conditions were used for dry and wet milling so that the results could be compared. In Table 1, the bold conditions are those for the lubricated machining experimental study. The first 10 conditions presented in Table 1 were used for constant identification (I1 to I5 for dry conditions and I6 to I10 for wet conditions). A complete experimental plan with three factors (cutting speed: five levels, feed: three levels, lubrication: two levels) was used to generate 30 combinations; these 30 tests will be used later for model validation. Finally, each test was repeated three times and the average value was retained.

Table 1 Experiments matrix

Test #	V_c, m/min	Feed, mm/tooth	Lubrication	Test #
I1	350	0.250	Dry/wet	**I6**
I2	450	0.075	Dry/wet	**I7**
I3	600	0.250	Dry/wet	**I8**
I4	700	0.100	Dry/wet	**I9**
I5	800	0.100	Dry/wet	**I10**
1	300	0.050	Dry/wet	**16**
2	400	0.050	Dry/wet	**17**
3	566	0.050	Dry/wet	**18**
4	733	0.050	Dry/wet	**19**
5	900	0.050	Dry/wet	**20**
6	300	0.125	Dry/wet	**21**
7	400	0.125	Dry/wet	**22**
8	550	0.125	Dry/wet	**23**
9	733	0.125	Dry/wet	**24**
10	900	0.125	Dry/wet	**25**
11	300	0.200	Dry/wet	**26**
12	400	0.200	Dry/wet	**27**
13	566	0.200	Dry/wet	**28**
14	733	0.200	Dry/wet	**29**
15	900	0.200	Dry/wet	**30**

3. Results and Discussions

For better readability and consideration of the effect of particle size on metallic dust concentration, the results are separated into two main sections: micrometer and nanometer size particles. Because different units are currently used in the literature to characterize particles (mass concentration, size distribution, specific surface, dust unit), this information is also provided.

3.1 Particle Mass Concentrations and Size Distribution

3.1.1 Microparticles. The influence of cutting conditions on particle mass concentration during milling processes for dry and wet milling is presented in Fig. 4. The particle mass concentration increases with increased cutting feed but decreases with the cutting speed. As illustrated in Fig. 4, the particle mass concentration is higher for wet machining than for dry machining for particles in the 0.5-1 μm size range. For this size range, the particle mass concentration is 5 to 30 times greater for wet than for dry milling. Nevertheless, for particle sizes between 1 and 10 μm, the mass concentration of particles generated in wet milling is much lower than the particle mass concentration in dry milling. It can be concluded that the cutting fluid was able to evacuate an important quantity of particles in the 1-10 μm size range. From the plotted results in Fig. 4, it can be concluded that the cutting fluid is unable to evacuate the particles with size less than 1 μm. In addition, the cutting fluid helps to generate particles with submicron size. These conclusions may be supported by observing the number of particles for wet and dry machining presented in Fig. 5.

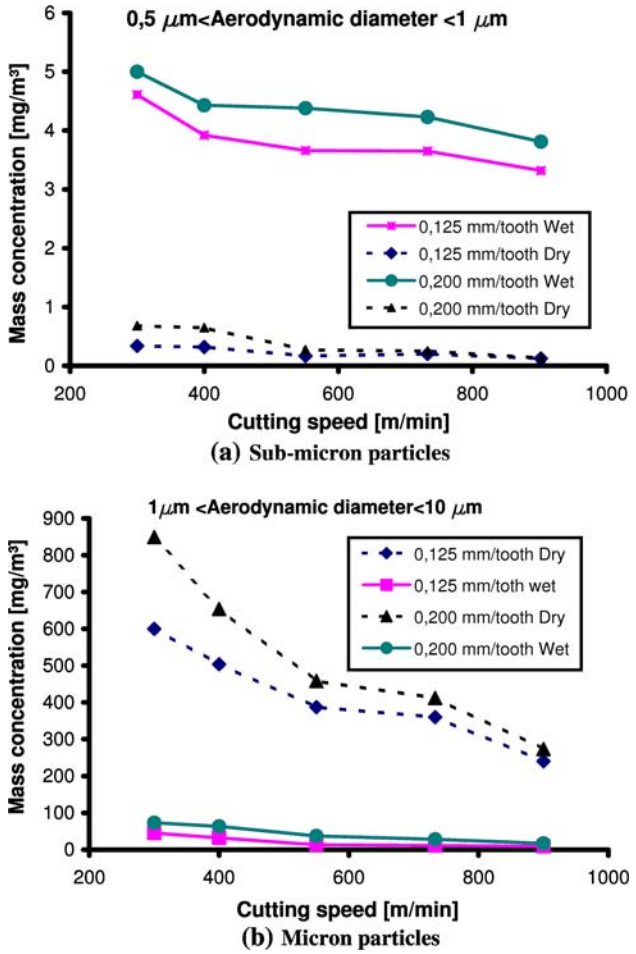

Fig. 4 Influence of the cutting speed on mass concentration for different particle sizes

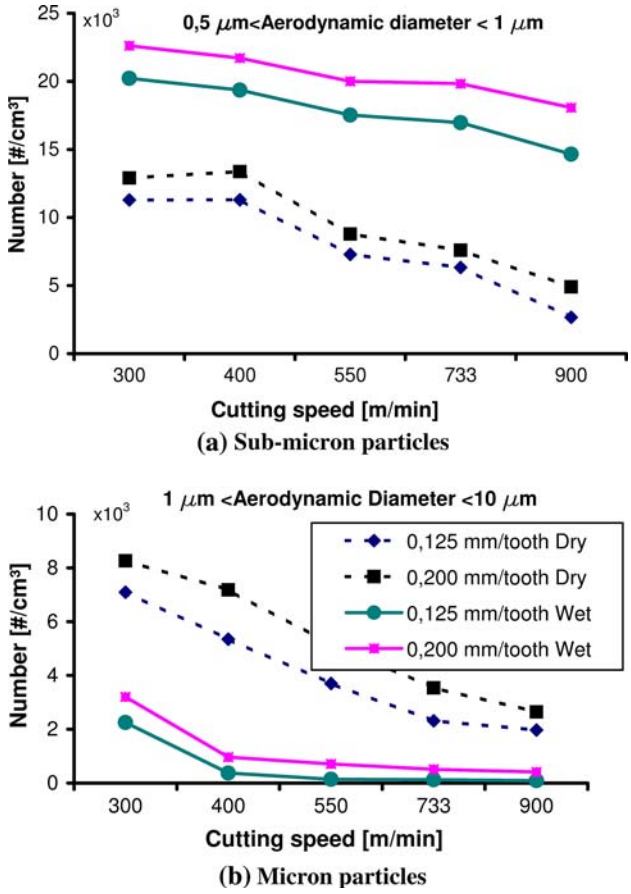

Fig. 5 Influence of the cutting speed on the particle number

In Fig. 5, the particle number for wet milling is 3 to 5 times higher than in dry milling. As the tests were conducted in the same cutting conditions, one may expect a higher number of particles for wet milling because of the mist created by the fluid impact. This was the case only for the submicron size range (0.5-1 micron). In fact, for this range (0.5-1 micron), the number of particles is two to five times higher in wet milling than in dry milling, while for the 1-10 μm size range the number of particles in dry milling is two to five times higher than in wet milling. Finally, the majority of particles generated during wet milling have a size range under 2.5 μm, especially when the cutting speed is moderate (see Fig. 6).

In Fig. 6, the particle size distribution was plotted for three particle size ranges (0.5-2.5, 2.5-10, and 10-20 μm). It can be concluded that increasing the cutting speed helps to reduce the generated dust in a dry milling process. The material softening in the chip formation zone explains this result. However, the material softening does not help the particles to separate from the chips. This conclusion can be supported by the experimental findings in (Ref 17). The authors found that the higher the material temperature, the lower the generated dust.

3.1.2 Nanoparticles. For nanoparticles, it is interesting to observe the nanoparticles specific surface in addition to the mass concentration, following the recommendations in Ref 12. It was shown also, that fine and ultrafine particle inhalation problems could be related to the particle-specific surface (Ref 11).

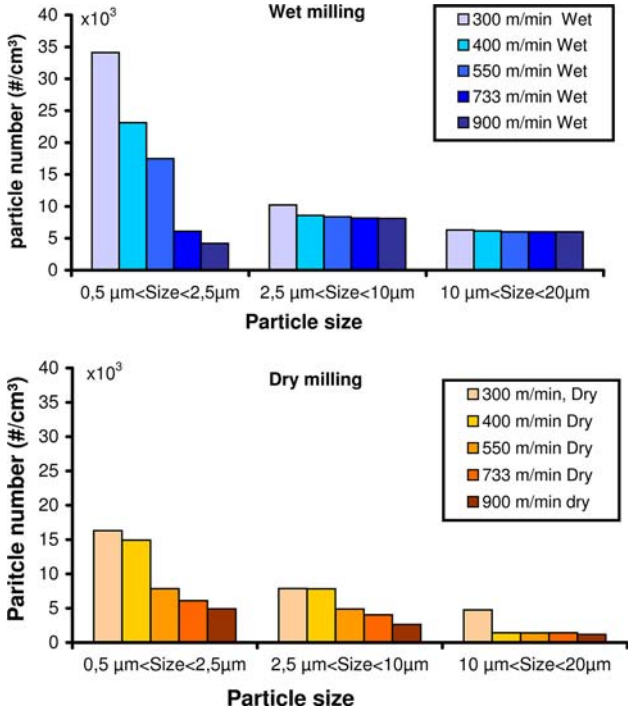

Fig. 6 Influence of the cutting speed on the particle size distribution for dry and wet milling

The instrumentation used during the present study is able to yield information necessary to investigate nanoparticles in the size range of 10-736 nm. A sample result is presented in Fig. 7 showing the information that can be collected after a machining test using the SMPS instrumentation. As expected, the released measurements show a non-negligible concentration and specific surface for nanoparticles in the range of 10-736 nm (Fig. 7b-d).

Following the work in Ref 9, the most harmful nanoparticles are the particles in the 10-20 nm size range. In Fig. 8, the nanoparticles concentration and specific surface are presented under different cutting conditions for dry and wet milling. Results are separated for two main size ranges, the 10-20 nm size range and the 20-736 nm size range.

In both dry and wet machining, a majority of the nanoparticles generated are in the 20-736 nm size range. The mass concentration of particles in this range is about 10,000 times higher than that of particles in the 10-20 nm size range (Fig. 8a, b). The specific particle surface follows a similar tendency (Fig. 8c, d).

The cutting speed and the feed do not significantly influence the generation of nanoparticles during wet milling (Fig. 8a-d); however, for dry milling, the influence of cutting speed is remarkable. The increase in cutting speed helps to reduce the nanoparticles concentration (Fig. 8a, b). The feed per tooth does not significantly affect the particle concentrations or the specific surface in either dry or wet conditions. As expected, the

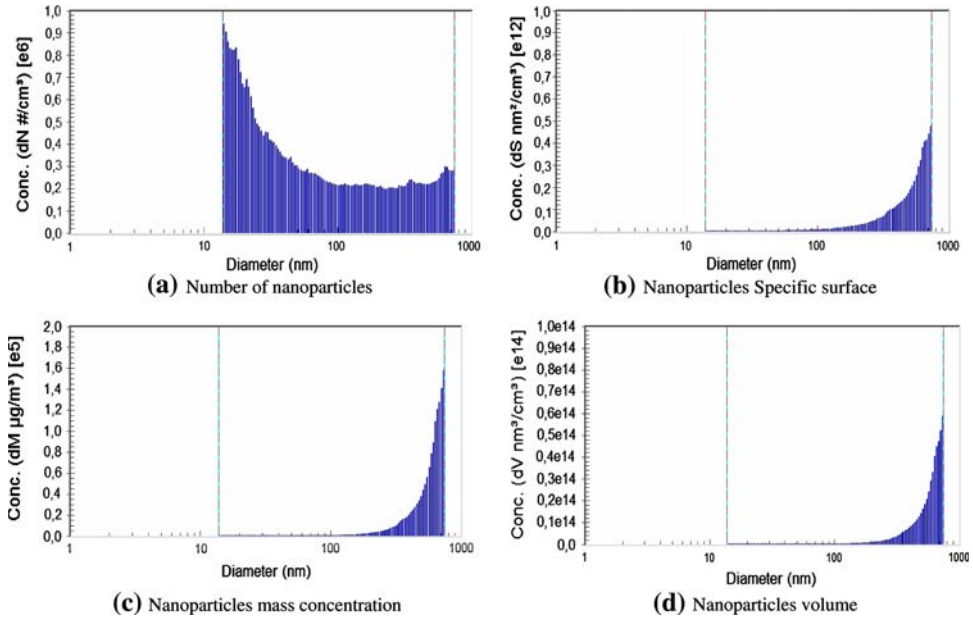

Fig. 7 Sample of collected results from the SMPS™ instrument

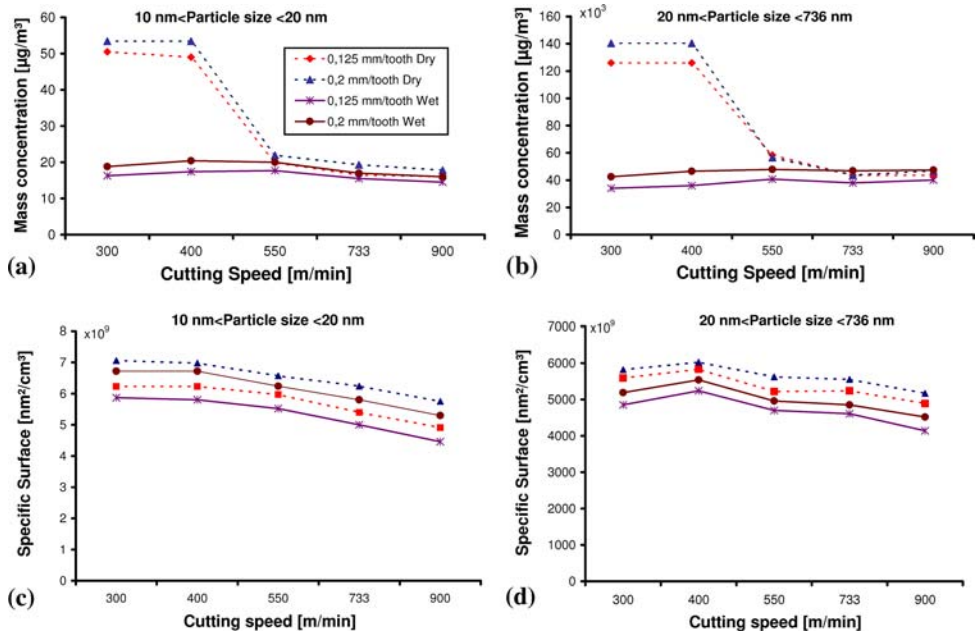

Fig. 8 Influence of cutting conditions on the nanoparticles mass concentration and specific surface

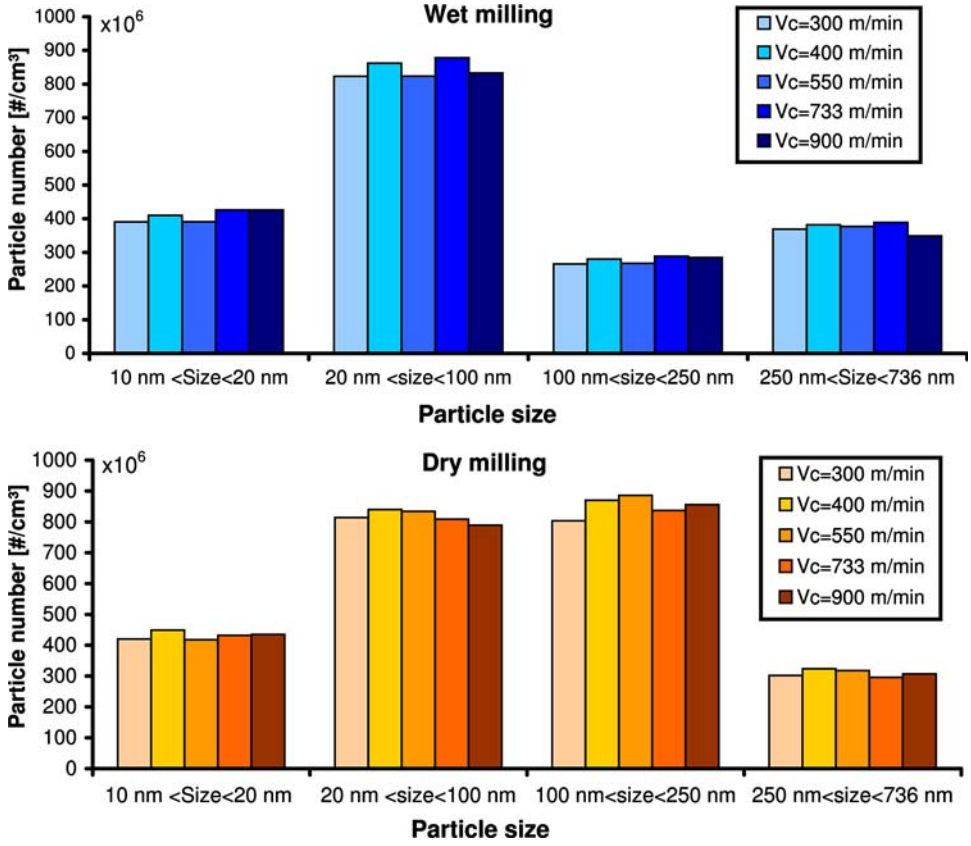

Fig. 9 Influence of the cutting speed on the nanoparticles size distribution for dry and wet milling

Table 2 Model constants for orthogonal milling of 6061-T6 aluminum alloy

	A	E_a, w/mm^2	m	Correlation coefficient R^2
Dry milling	25×10^{-4}	158	70×10^{-3}	99.8%
Wet milling	2.4×10^{-4}	517	5×10^{-3}	99.6%

lubrication has no significant influence on nanoparticles specific surface. The lubricant is not able to split or evacuate nanoparticles.

Figure 9 shows that for the four ranges of particle sizes, the number of nanoparticles remains mainly constant with the exception of particles in the 100-250 nm size range. The number of particles for this size was about two times higher in wet conditions (Fig. 9a) than in dry conditions (Fig. 9b), although no explanation was found for this behavior. For other range sizes, the same particle number was obtained during dry and wet milling for the most part. This conclusion supports previous results concerning the non-effect of lubricant on nanoparticles generation.

3.2 Model Validation

The proposed model for prediction of dust generation during a milling process is based on the energy approach for an orthogonal milling process. To use the developed equations for an orthogonal process, the plane strain condition should be verified first. For each machining test, the collected chips were measured under an optical microscope. It was observed that the width of the chip w (see Fig. 3) is mainly constant for all cutting conditions. This result means that there is no deformation in the axial direction. Therefore, the plane strain condition is fulfilled and Eq 1-6 presented in section 2.1 can be applied to the investigated process. The constants A, E_a, and m in Eq 3 were identified using the Levenberg-Marquadt algorithm, which is widely used for nonlinear problem identification. The results for model identification for dry and wet milling tests are presented in Table 2. As the correlation factor, R^2, is higher than 90%, the derived relations can be considered reliable and the coefficients can be used for further analysis.

The activation energy, E_a, for dry milling is lower than the activation energy for wet milling. This means that fine and ultrafine particles can detach more easily in dry than in wet milling. The cooling removes the heat from the chip formation zone; therefore, more energy is required to separate the particle from the parent material. Knowing that the cutting fluid will take out a large part of this energy may explain why the activation energy E_a is found to be higher in wet than in dry conditions.

The constant A is related mainly to the friction conditions in the tool-chip interface (Ref 3), and is ten times greater in dry than in wet milling. This result can be explained by the severe interface conditions observed in dry machining processes. The energy rate per unit area, E_s, generated in the chip formation zone was estimated from the measured cutting forces and the measured chip compression ratio C_h. For the investigated cutting conditions, it was found that E_s is higher in dry than in wet milling processes.

Once the constants A, E_a, and m are identified and the energy E_s is computed, the percentage of the generated dust can be calculated using Eq 4. The prediction is compared to the experimental measurement for dry and wet conditions, and the results are presented in Fig. 10-12. Good agreement between the model and experimental results is observed for the investigated conditions. The model predicts that the percentage of generated dust D_u will decrease with the cutting speed (Fig. 11).This confirms results already obtained during the turning process (Ref 3). It can be concluded that high-speed cutting can reduce dust emission for the milling process of aluminum alloys, and material softening explains this result. In fact, the higher the created energy in the chip deformation zone, the fewer particles will separate from the formed chip (Fig. 10). Results for generated dust were presented versus the measured chip compression ratio. As expected, it was found that the generated dust increases with the chip compression ratio.

From the comparison between predicted and measured dust (Fig. 10-12), it can be concluded that the shearing zone is the main source of dust emission. In fact, the proposed model, which is based on an energy approach in the primary shear zone, was able to explain most of the experimental results.

The deformation conditions in the primary shear zones were studied for their influence on dust generation. The average shear strain , $\bar{\gamma}_{prim}$, in the primary shear zone is calculated using the following equation (Ref 28)

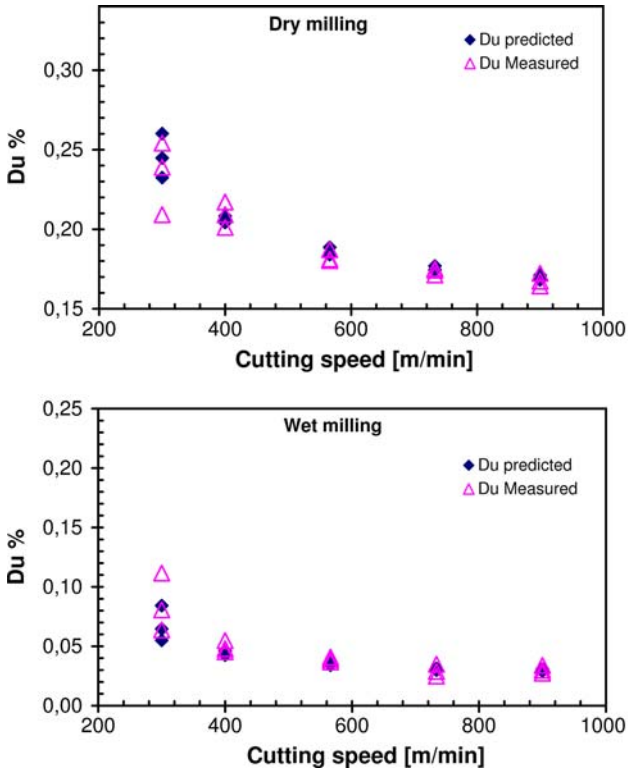

Fig. 11 Effect of cutting speed on predicted and measured dust generation

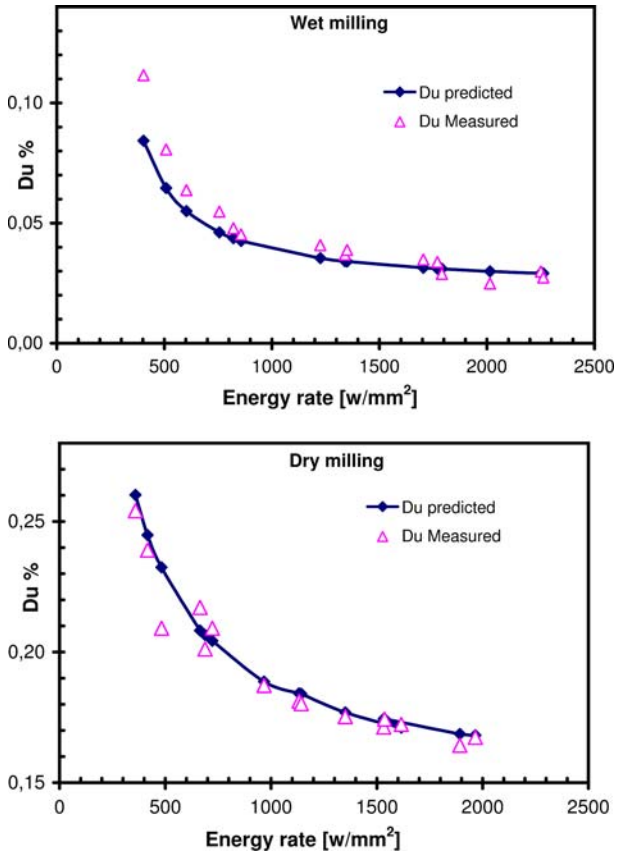

Fig. 10 Comparison between prediction and measurement of dust generation for dry and wet milling

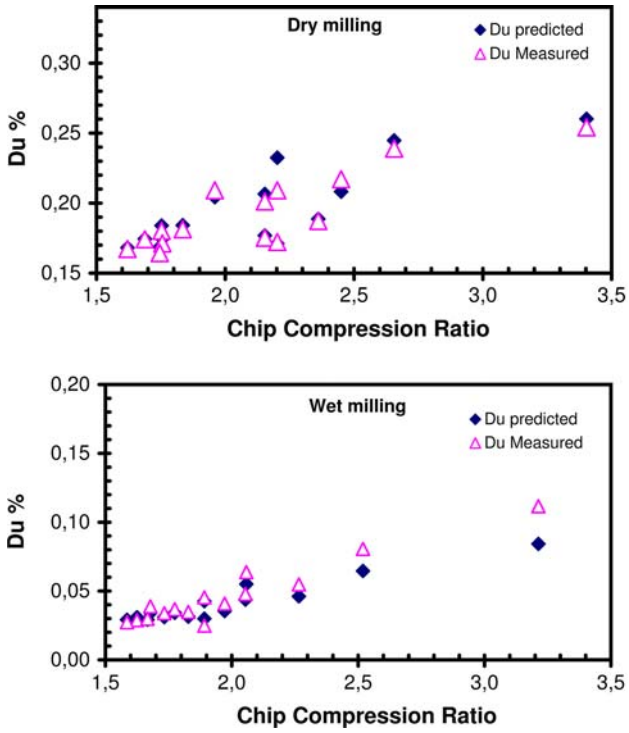

Fig. 12 Effect of chip compression ratio on predicted and measured dust generation

$$\bar{\gamma}_{\text{prim}} = \frac{\cos \alpha_n}{2 \cos(\phi - \alpha_n) \sin \phi} \quad \text{(Eq 7)}$$

where ϕ is the shear angle and α_n is the tool rake angle. The influence of the shear strain on dust generation is presented in Fig. 13 for dry and wet conditions. The percentage of the generated dust increases with the shear strain. This can be explained by the high energy that can be created due to high deformation: the more energy in the chip formation zone, the higher the percentage of generated dust. The chip formation zone energy depends widely on the cutting conditions and the work piece material, and deeply influences chip morphology. The morphologies of the generated chips for different cutting conditions are presented in Fig. 14. At a microscopic scale, the chip is formed from serrated microbands. These microbands become more serrated with increases in feed and speed. The lubrication mode has an influence on chip morphology as well. It is found that at low cutting speed, there is no significant difference in the microband density between wet and dry milling. At high speed, the microband densities for wet and dry milling are significantly different. Dry machining produces larger and more widely spaced microbands. This morphology helps particles to detach more easily from the chip and causes more dust generation during dry milling processes.

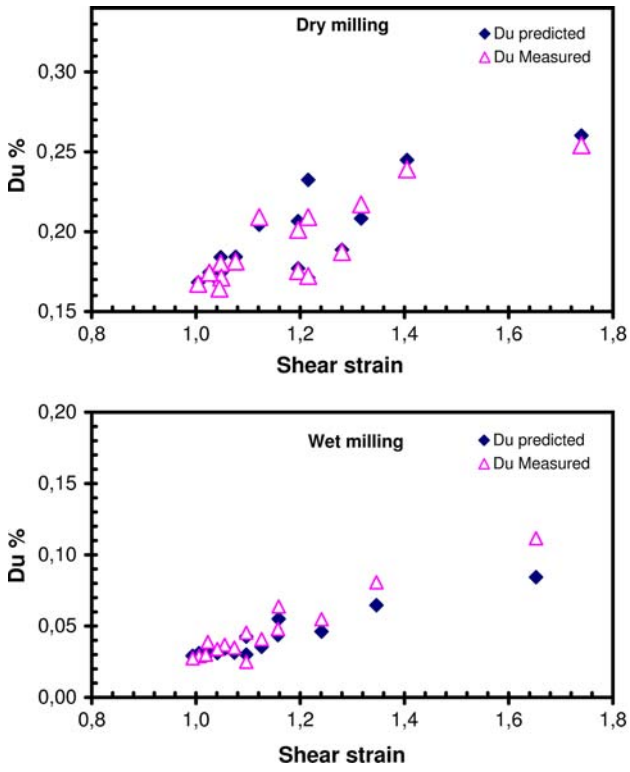

Fig. 13 Effect of shear strain on predicted and measured dust generation

Not only the deformation influences the generated dust, but the shear strain rate also has an influence. Many authors have demonstrated the effect of strain rate in metal cutting and the relation between strain rate and cutting conditions (e.g., Ref 29). The following equation was used to compute the average shear strain rate ($\dot{\bar{\gamma}}_{\text{prim}}$)

$$\dot{\bar{\gamma}}_{\text{prim}} = \frac{2 V_c \cos \alpha_n}{e_{\text{psz}} \cos(\phi - \alpha_n)} \quad \text{(Eq 8)}$$

where e_{psz} is the width of the primary shear zone estimated using Oxley's approximation of the tenth of the feed per tooth, V_c is the cutting speed, ϕ the shear angle and α_n the tool rake angle. The relation between the shear strain rate and the generated dust is presented in Fig. 15. The percentage of the generated dust decreases with the strain rate for the tested feeds. It can be concluded that the generated dust is significantly influenced by the deformation conditions in the primary shear zone. This factor should be considered during any

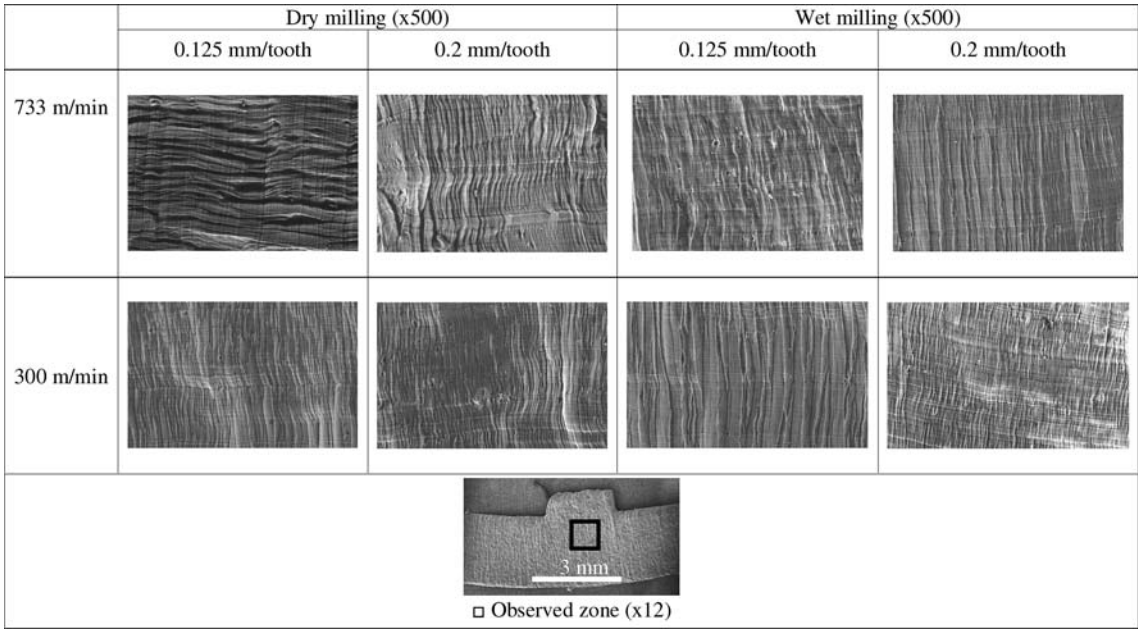

Fig. 14 Chip aspect and morphology for different cutting conditions

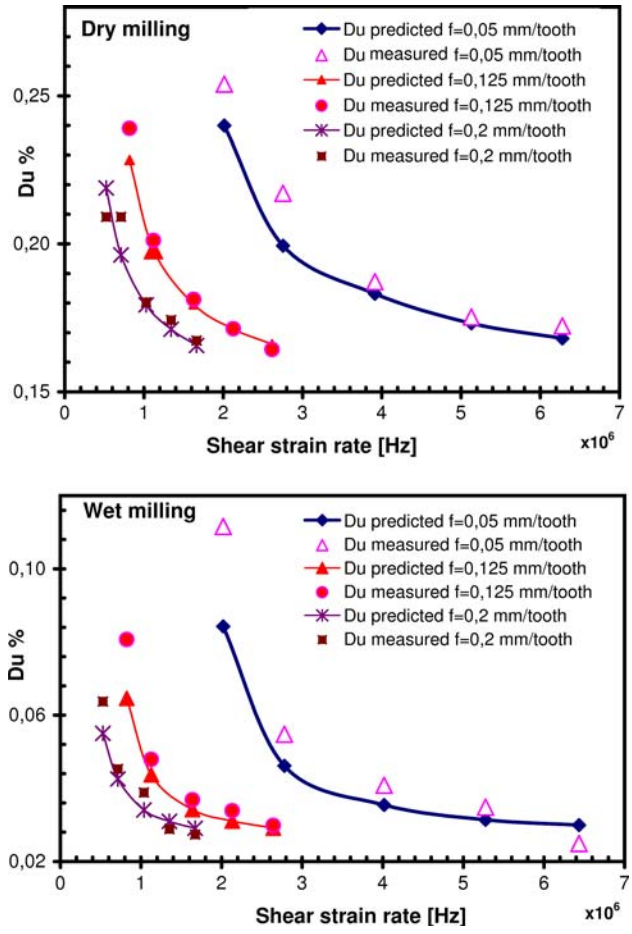

Fig. 15 Effect of shear strain rate on predicted and measured dust generation

test for evaluation of the material dust emissivity. The test deformation conditions should be similar to machining deformations conditions that are high in strain and in strain rate. In Fig. 5, the percentage of generated dust is presented for three feeds, and it is found that the percentage of the dust is inversely proportional to the chip thickness. The observed results are consistent with experimental findings made by Palmqvist and Gustafsson (Ref 18) and confirmed by Rautio et al. (Ref 19) for wood milling.

4. Conclusions

From the experimental measurements and observations for dust generation during an orthogonal machining process, it can be concluded that:

1. The dust generation is in direct relation with the generated energy in the chip formation zone and the dust generation decreases with the energy rate per area. Lubrication affects the form of most generated particles and has no effect on nanoparticles emission. Wet milling processes produce more particles than dry milling processes for the submicron size range. For a particle in the 1-10 μm size range, the dry milling process produces more particles than the wet milling process. The cutting fluid and the cutting conditions do not have a major influence on nanoparticles specific surface and size distribution.
2. The cutting speed and feed per tooth have no significant influence on the nanoparticles mass concentrations for wet milling; nevertheless, the cutting speed significantly influences the nanoparticles mass concentration for dry milling.
3. There is a strong indication that the shearing zone is the main source of dust emission during machining. The proposed model considers the shear velocity, the shear stress, the shear angle, and the chip compression ratio, and explains most of the observed experimental results. It is found that generated dust is significantly influenced by the deformation conditions (strain and strain rate) in the chip formation zone.
4. The model showed good agreement with experimental measurements for the investigated conditions. The observed results were consistent with existing findings concerning dust generation during machining processes.
5. The proposed model is limited to microparticles and is not suitable for nanoparticles dust generation because the cutting conditions do not much influence the generation of nanoparticles.

References

1. L. Gradus and Y. Popov, Methods of Decontaminating Emissions During Machining of Materials, *Khim. Neft. Mashinostr.*, 1984, **2**, p 10–11
2. H. Tönshoff, B. Karpuschewski, and T. Glatzel, Particle Emission and Emission in Dry Grinding, *Ann. CIRP*, 1997, **46**(2), p 693–695
3. R. Khettabi, V. Songmene, and J. Masounave, The Effect of Tool Geometry and Cutting Parameters on Dust Emission During Dry Machining, *J. Mater. Process. Technol.*, 2007, **194**(1–3), p 100–109
4. J.W. Sutherland, V.N. Kulur, and N.C. King, An Experimental Investigation of Air Quality in Wet and Dry Turning, *Ann. CIRP*, 2000, **49**, p 61–64
5. M. Ramulu, P. Young, and H. Kao, Drilling of Graphite/Bismaleimide Composite Material, *J. Mater. Eng. Perform.*, 1999, **8**, p 330–338
6. V. Songmene, J. Masounave, and B. Balout, Clean Machining: Experimental Investigation on Dust Formation Part I: Influence of Machining Parameters and Chip Formation, Part I, *Int. J. Environ. Conscious Des. Manuf. (ECDM)*, 2008, **14**(1), p 1–16
7. V. Songmene, J. Masounave, and B. Balout, Clean Machining: Experimental Investigation on Dust Formation Part I: Influence of Machining Parameters and Chip Formation, Part II, *Int. J. Environ. Conscious Des. Manuf. (ECDM)*, 2008, **14**(1), p 17–33
8. F.P. Holt, *Inhaled Dust and Disease*. John Wiley & Sons, New York, 1987
9. O. Witschger and F. Fabriès, Particules ultra-fines et santé au travail 1 – caractéristiques et effets potentiels sur la santé, *INRS*, 2005, **199**, p 21–35 (http://www.inrs.fr/htm/particules_ultra-fines_sante_travail.html) (in French)
10. Q. Zhang, Y. Kusaka, and K. Donaldson, Comparative Pulmonary Responses Caused by Exposure to Standard Cobalt and Ultra Fine Cobalt, *J. Occup. Health*, 2000, **42**, p 179–184
11. G. Oberdörster, E. Oberdörster, and J. Oberdörster, Nanotechnology: An Emerging Discipline Evolving from Studies of Ultra Fine Particles, *Environ. Health Perspect.*, 2005, **113**(7), p 823–839
12. C. Ostiguy, G. Lapointe, L. Ménard, Y. Cloutier, M. Trottier, M. Boutin, M. Antoun, and C. Normand, Les nanoparticules : État des connaissances sur les risques en santé et sécurité du travail, *IRSST*, 2006, (http://www.irsst.qc.ca/files/documents/PubIRSST/R-455.pdf) (in French)
13. G. Kreyling, M. Semmler, F. Erbe, P. Mayer, S. Takenaka, H. Schultz, G. Oberdoster, and A. Ziesenis, Translocation of Ultra Fine Insoluble Iridium Particles from Lungs Epithelium to Extra Pulmonary Organs, *J. Toxicol. Environ. Health*, 2002, **65**(20), p 1513–1530

14. C. Katz, A. Burkhalter, and W. Dreyer, Fluorescent Latex Micro Spheres as a Retrograde Neuronal Marker for In Vivo and In Vitro Studies of Visual Cortex, *Nature*, 1984, **310**, p 498–500
15. A. Gatti, Biocompatibility of Micro and Nanoparticles in the Colon. Part II, *Biomaterials*, 2004, **25**(3), p 385–392
16. A.C. Elder, R. Gelein, M. Azadniv, M. Frampton, J. Finkelstein, and G. Oberdorster, Systemic Effects of Inhaled Ultra Fine Particles in Two Compromised, Aged Rat Strains, *Inhale Toxicol.*, 2004, **16**, p 461–471
17. B. Balout, V. Songmene, and J. Masounave, An Experimental Study of Dust Generation During Dry Drilling of Pre-cooled and Pre-heated Work Piece Materials, *J. Manuf. Process.*, 2007, **9**, 23–34
18. J. Palmqvist and S. Gustafsson, Emission of Dust in Planning and Milling of Wood, *Holz. Roh Werkstoff*, 1999, **57**, p 164–170
19. S. Rautio, P. Hynynen, I. Welling, I. Hemmil, P. Usenius, and A. Narhi, Modelling of Airborne Dust Emissions in CNC MDF Milling, *Holz. Roh Werkstoff*, 2007, **65**(7), p 335–341
20. R. Khettabi, "Modélisation prédiction et réduction des émissions de poussière au cours de l'usinage," Ph.D. thesis, University of Québec, École de Technologie Supérieure, Montréal, Canada, 2008 (in French)
21. J. Xie, A. Bayoumi, and H. Zbib, A Study on Shear Banding in Chip Formation of Orthogonal Machining, *Int. J. Mach. Tools Manuf.*, 1996, **36**(7), p 835–847
22. E. Merchant, Mechanics of the Metal Cutting Process, Part I: Orthogonal Cutting and Type 2 Chip, *J. Appl. Phys.*, 1945, **16**(5), p 267–275
23. W. Hastings, P.L.B. Oxley, and M. Stevenson, Predicting a Material's Machining Characteristics Using Flow Stress Properties Obtained from High-Speed Compression Tests, *Proceedings of Mechanics Engineering*, 1974, **188**, p 245–252
24. N. Tounsi, J. Vincenti, A. Otho, and M. Elbestawi, From the Basic Mechanics of Orthogonal Metal Cutting Toward the Identification of the Constitutive Equation, *Int. J. Mach. Tools Manuf.*, 2002, **42**(12), p 1373–1383
25. TSI Inc., Operation and Service Manual, Model 3321 Model 3321 Aerodynamic Particle Sizer® Spectrometer, Revision E, 2004, p 1–3
26. TSI Inc., Operation and Service Manual, Series 3080 Electrostatic Classifiers, Revision H, 2008, p 1–4
27. TSI Inc., Operation and Service Manual, Model 3786 Ultra Fine Water Based Condensation Particle counter, Revision B, 2005, p 1–3
28. V. Astakhov and S. Shvets, The Assessment of Plastic Deformation in Metal Cutting, *J. Mater. Process. Technol.*, 2004, **146**, p 193–202
29. P.L.B. Oxley, *Mechanics of Machining: An Analytical Approach to Assessing Machinability.* Ellis Horwood Limited, 1989